Petroleum Science 23 (2026) 3459–3471

Contents lists available at ScienceDirect

Petroleum Science

journal homepage: www.keaipublishing.com/en/journals/petroleum-science

Original Paper

Mechanisms of miscible gas injection for ultra-low permeability carbonate reservoirs: A case study of the S reservoir in the H oilfield, Iraq

Zhou-Hua Wang [a,*], Xin-Tong Zhang [a], Guang-Ya Zhu [b], Ping Guo [a], Nan Li [b], Hui Liu [b], Zhao-Ming Li [a], Huang Liu [a], Shuo-Shi Wang [a]

[a] State Key Laboratory of Oil and Gas Reservoir Geology and Exploitation, Southwest Petroleum University, Chengdu, 610500, Sichuan, China
[b] Research Institute of Petroleum Exploration and Development, Beijing, 100083, China

A R T I C L E I N F O

Article history:
Received 1 April 2025
Received in revised form
7 November 2025
Accepted 25 February 2026
Available online 3 March 2026

Edited by Meng-Jiao Zhou

Keywords:
Porous carbonate
Extra-low permeability
Miscible gas drive
Utilization degree
Gas injection parameter

A B S T R A C T

The S reservoir is a typical Middle Eastern carbonate formation characterized by a formation temperature of 89 °C, salinity of 200,000 mg/L, and permeability below 1 mD. It exhibits low and continuously declining formation pressure and single-well productivity, making water flooding inefficient. Therefore, it is essential to evaluate the feasibility of gas injection to supplement reservoir energy and provide a theoretical basis for selecting suitable injection media and parameters for field development. To address these challenges, a high-temperature and high-pressure NMR online gas displacement and long-core flooding experimental system was established. Gas expansion, minimum miscibility pressure, and dynamic core displacement experiments were conducted and integrated with numerical simulations to examine the effects of gas type, injection timing, and injection rate on microscopic displacement behavior, recovery efficiency, and flow characteristics in ultra-low-permeability carbonate reservoirs. The results indicate that, in such tight formations, macroscopic flow follows non-Darcy behavior with a distinct threshold pressure gradient, while microscopically, gas diffusion from larger pores into smaller throats promotes oil displacement. The coupling between molecular diffusion and the threshold pressure gradient jointly governs ultimate recovery efficiency, providing new insights into gas injection mechanisms in ultra-low-permeability carbonate reservoirs. Experimental findings further demonstrate that crude oil in the S reservoir exhibits a large saturation pressure difference and low viscosity. Gas injection enhances the elastic expansion capacity of crude oil by 13.68%–19.54% and reduces its viscosity by 8.08%–12.23%. Under the current formation pressure (34.45 MPa), CO_2 and hydrocarbon gas achieve miscible flooding, whereas N_2 remains immiscible. Miscible flooding improves small-pore oil utilization by approximately 20%, and considering both miscibility and displacement efficiency, hydrocarbon gas is recommended as the preferred injection medium. Compared with N_2 immiscible flooding, hydrocarbon gas—under pulse or continuous injection—achieves more than 50% recovery. The optimal conditions for miscible flooding include an injection rate of 0.0811–0.0908 m/d, injection pressure above the MMP, and an injection–production ratio of 1:1, resulting in a maximum recovery efficiency of up to 76%. This study establishes both a theoretical and experimental foundation for optimizing gas injection in ultra-low-permeability carbonate reservoirs and demonstrates practical relevance by improving gas–oil mobility control, reducing emulsion stability, and enhancing separation efficiency during surface fluid processing.

1. Introduction

The S reservoir in the H oilfield accounts for approximately 25% of the field's geological reserves and serves as a key target for production replacement. It is a typical ultra-low-permeability porous carbonate reservoir characterized by low structural

* Corresponding author.
E-mail address: wangzhouhua@126.com (Z.-H. Wang).
Peer review under the responsibility of China University of Petroleum (Beijing).

https://doi.org/10.1016/j.petsci.2026.02.021
1995-8226/

amplitude and strong heterogeneity (Yang et al., 2022a, 2022b). Vertically, the reservoir is divided into two formations, S-B and Tanuma, with no observed edge or bottom water. The porosity ranges from 14.00% to 20.00%, and the permeability varies from 0.01×10^{-3} to 5.00×10^{-3} μm^2. The formation crude oil has a viscosity of 0.451 mPa s, classifying it as a low-viscosity medium crude oil. Due to the poor reservoir quality, single-well production rates are low, production declines rapidly, and water injection remains challenging. Consequently, it is imperative to evaluate gas injection as a potential method to enhance recovery efficiency in this reservoir.

Ultra-low-permeability carbonate reservoirs are primarily developed through three approaches: depletion, waterflooding, and gas injection (Mogensen and Masalmeh, 2020; Mohammadi et al., 2022; Song and Li, 2018; Song et al., 2024a; Su and Liao, 2014; Sun et al., 2022; Wang et al., 2020; Zhang et al., 2021). In the San Andres oilfield of the United States, early depletion development yielded limited success because strong reservoir heterogeneity resulted in high residual oil saturation after primary recovery, leaving a large portion of crude oil unrecovered (Yang et al., 2017). Al-Murayri et al. (2019) conducted a laboratory feasibility study on low-salinity and polymer flooding in a low-permeability carbonate reservoir in Kuwait. The waterflooding efficiency achieved with low-salinity water reached up to 70%, and the addition of polymer further enhanced the recovery efficiency to 82%.

Water injection in ultra-low-permeability carbonate reservoirs often suffers from low imbibition efficiency, poor injectivity, and formation damage (Yu et al., 2019), thereby rendering gas injection a more favorable development approach for such reservoirs. Compared with waterflooding, gas injection can more readily establish an effective displacement pressure system, significantly reduce interfacial tension (IFT), and enhance oil swelling and viscosity reduction effects (Choubineh et al., 2019; Han et al., 2015, 2018; Hu et al., 2018; Ju et al., 2012; Liu et al., 2017; Liu and Chen, 2010; Wan and Liu, 2018; Yuan et al., 2020; Zhu et al., 2021). Gas flooding can be categorized into two types: immiscible and miscible displacement. Immiscible displacement primarily utilizes the expansion energy of injected gas to quickly establish a pressure system, displacing crude oil in the pores and increasing recovery. However, in strongly heterogeneous reservoirs, two-phase coexistence within the pore space promotes gas channeling, resulting in limited incremental recovery during area-wide displacement. In contrast, miscible flooding eliminates the phase interface entirely, reduces IFT to near zero, mobilizes crude oil trapped in small throats, and effectively delays gas channeling. Its combined effects of oil swelling and viscosity reduction substantially improve crude oil mobility and overall recovery efficiency.

Keyvani and Safaei et al. (Keyvani et al., 2024; Li et al., 2022; Safaei et al., 2021) further emphasized that the efficiency of miscible gas flooding strongly depends on achieving complete phase contact, as well as on diffusion and mass-transfer processes that govern miscibility development and displacement stability. Their findings demonstrated that molecular diffusion between injected gas and crude oil accelerates component exchange, sustains phase equilibrium, and enhances sweep efficiency in both carbonate and tight formations. These insights provide theoretical support for understanding the miscible flooding behavior discussed in this study. Similarly, Tan et al. (2022) systematically investigated the mechanisms of CO_2–enhanced oil recovery (EOR) in carbonate reservoirs and concluded that, in addition to the extraction of light components, reducing IFT, and improving oil swelling and viscosity reduction, CO_2 diffusion and mass transfer in crude oil are also key mechanisms controlling recovery performance. Liu et al. (2013) experimentally evaluated the feasibility of associated gas injection in a Middle Eastern porous carbonate reservoir and found that gas injection improved crude oil mobility through swelling and viscosity reduction, achieving a displacement efficiency of 52.02%. Likewise, Figuera et al. (2016) and Deinum et al. (Deinum et al., 2007; Al-Hadhrami et al., 2007) investigated CO_2 and hydrocarbon gas injection in the Abu oilfield and the A reservoir of the Harweel field, respectively, demonstrating that miscible gas flooding significantly enhanced crude oil mobility and increased the recovery factor by more than 20%.

Numerical and physical simulations are the primary approaches for evaluating development strategies in extra-low-permeability carbonate reservoirs. Saadawi (2010) employed numerical simulation to assess the performance of various development strategies—namely, waterflooding and gas injection—and different injection parameters, including injectant type and injection mode, in typical ultra-low-permeability carbonate reservoirs. They concluded that waterflooding in such reservoirs encounters major challenges, such as injection difficulties and pronounced crude oil degassing, resulting in unsatisfactory development performance. In contrast, gas injection maintains reservoir pressure, reduces viscosity, improves crude oil mobility, and enhances incremental oil recovery, increasing the recovery factor by 15%–19%. In addition, numerous researchers have conducted miscible flooding experiments on carbonate reservoirs using various injection media and methods. For example, Shi et al. (2017) investigated a low-permeability carbonate reservoir in the Middle East using NMR to examine the displacement efficiency differences under different waterflooding schemes in heterogeneous reservoir layers. They found that recovery efficiency varied significantly between layer-by-layer and simultaneous injection–production modes. After waterflooding, residual oil mainly existed as oil films in large pores, while small pores were occupied by bound water. Li et al. (2020) addressed the challenges of strong heterogeneity and unreliable forecasting in large, thick carbonate reservoirs by classifying vertical stacking patterns of reservoir layers and integrating them into injection well network designs. They developed type curves for waterflooding in different stacking configurations, substantially improving prediction efficiency. Wei et al. (2022) focused on issues such as gas channeling, high gas–oil ratios, and inefficient gas recycling observed during more than a decade of miscible hydrocarbon gas injection in a typical Middle Eastern low-permeability carbonate reservoir. Through numerical simulation, they proposed a comprehensive evaluation framework for miscible gas flooding performance, identified key factors influencing gas channeling, and developed optimization strategies to improve injection efficiency. Al-Hajeri et al. (Al-Hajeri et al., 2010; Salma et al., 2011), Al-Riyamy et al. (2005), and Abedini et al. (2015) combined core flooding experiments with numerical simulations to investigate enhanced oil recovery performance in low-permeability carbonate reservoirs using CO_2 and hydrocarbon gas injection. Their results indicated that these reservoirs can achieve substantial incremental recovery before gas breakthrough, with continuous gas injection maintaining high reservoir pressure and significantly prolonging the stable production period. However, despite extensive experimental and numerical research, the underlying mechanisms governing miscible gas displacement in ultra-low-permeability carbonate reservoirs remain insufficiently understood.

In summary, both field experience and numerical studies have demonstrated that gas injection represents a more effective development strategy for ultra-low-permeability carbonate reservoirs. To address the challenges identified above, this study established a high-temperature and high-pressure NMR online gas displacement and long-core flooding experimental system. Gas flooding simulation experiments were performed to investigate the effects of different injection media and parameters on microscopic displacement behavior, recovery efficiency, and flow characteristics in ultra-low-permeability carbonate reservoirs by integrating laboratory experiments with numerical simulations. The results show that, in such tight formations, macroscopic fluid flow is dominated by non-Darcy behavior with a distinct threshold pressure gradient, while at the microscopic scale, gas diffusion from larger pores into smaller throats drives oil displacement. The coupling between molecular diffusion and the threshold pressure gradient jointly controls ultimate recovery efficiency, providing new insights into gas injection mechanisms in ultra-low-permeability carbonate reservoirs (Fig. 1).

2. Experimental conditions and testing methods

2.1. Experimental materials

2.1.1. Fluid samples

Based on the PVT data of formation fluids from representative wells in the study area, the original reservoir oil was reconstituted by mixing degassed crude oil and separator gas under initial reservoir conditions (pressure: 34.45 MPa, temperature: 89 °C, and gas–oil ratio (GOR): 209.20 m^3/m^3), in accordance with relevant industry standards. The measured saturation pressure of the reconstituted oil sample was 24.51 MPa, with a single-stage degassed GOR of 204.63 m^3/m^3 and a viscosity of 0.458 mPa·s at the saturation pressure. These parameters closely match those of the original reservoir fluids, confirming the accuracy of the reconstitution process. The compositions of the reconstituted reservoir crude oil and the injected gases are summarized in Table 1.

The hydrocarbon gas used for injection was formulated based on the PVT report (Table 1), whereas N_2 and CO_2 were commercial-grade gases with a purity of 99.00%. Before conducting long-core and NMR displacement experiments, gas injection expansion tests and slim-tube tests were carried out to systematically evaluate the effects of gas injection on the high-pressure physical properties of formation fluids and to determine the miscibility between the injected gases and crude oil. The results of the gas injection expansion tests (Table 2) show that as the injected gas volume increased, the elastic expansion capacity of the crude oil improved while its viscosity decreased, demonstrating a clear enhancement of fluid mobility. Under reservoir conditions (pressure: 34.45 MPa, temperature: 89 °C), the minimum miscibility pressures (MMPs) obtained from the slim-tube tests were 45.00 MPa for N_2, 30.20 MPa for CO_2, and 31.20 MPa for hydrocarbon gas (Fig. 2). Therefore, under the current reservoir conditions, N_2 injection corresponds to immiscible flooding, whereas CO_2 and hydrocarbon gas injections achieve miscible flooding.

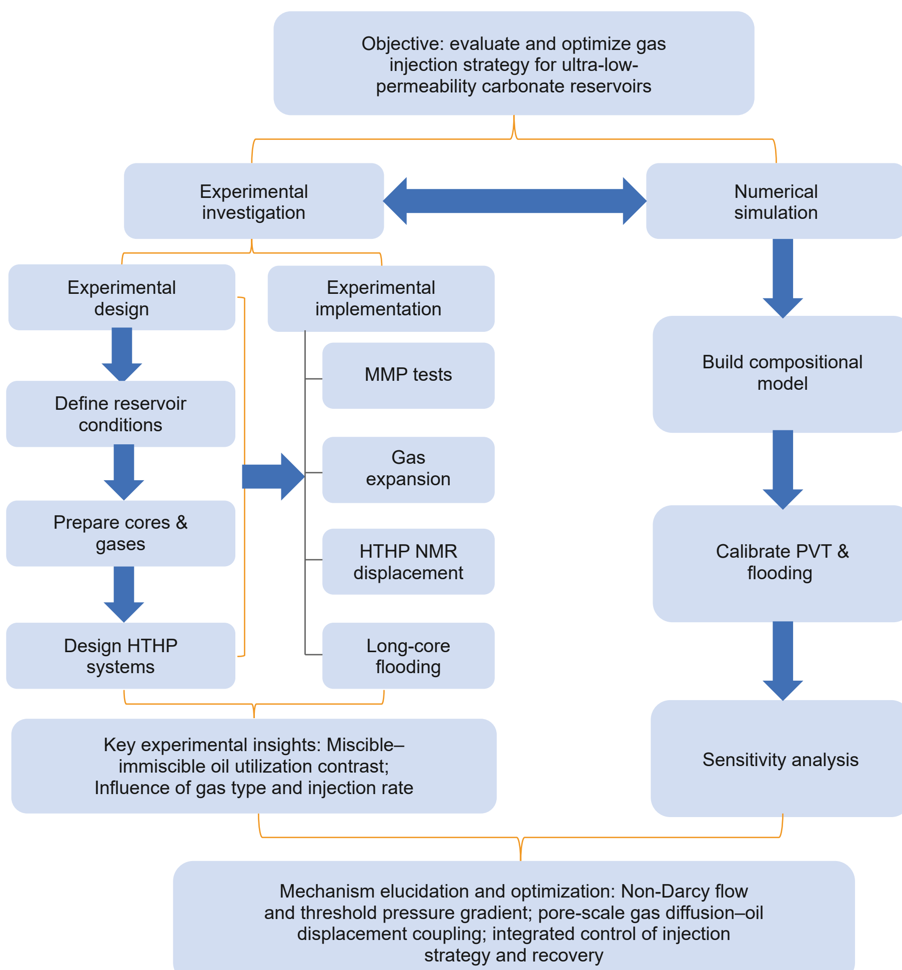

Fig. 1. Research workflow illustrating the experimental design, implementation, and numerical simulation processes used to investigate gas flooding mechanisms and optimize injection strategies in ultra-low-permeability carbonate reservoirs.

Table 1
Composition of blended reservoir crude oil and injected gases.

Components	Molar fraction of formation crude oil components, %	Molar composition of the injected hydrocarbon gas, %
CO_2	0.49	2.83
N_2	0.11	0.01
C_1	37.18	64.62
C_2	11.56	16.57
C_3	9.64	14.02
iC_4	1.39	0.60
nC_4	1.64	0.59
iC_5	2.07	0.54
nC_5	1.99	0.10
C_6	5.96	0.12
C_{7+}	27.97	/

Table 2
Results of gas injection expansion tests.

Injection medium	Molar fraction of gas injection, %	GOR, m^3/m^3	Saturation pressure, MPa	Volume coefficient	Expansion coefficient	Density, g/cm^3	Viscosity, cP
/	0.00	205.20	24.55	1.5993	1.0000	0.6944	0.458
N_2	4.44	220.02	27.17	1.6450	1.0258	0.6903	0.449
	9.09	238.50	32.14	1.6863	1.0531	0.6874	0.442
	14.01	260.26	36.62	1.7347	1.0809	0.6825	0.436
	19.29	286.52	42.17	1.8010	1.1065	0.6767	0.427
	24.55	316.34	46.90	1.8480	1.1368	0.6731	0.421
CO_2	5.37	223.60	25.52	1.6554	1.0356	0.6881	0.447
	9.76	241.34	26.48	1.7397	1.0686	0.6825	0.435
	14.89	264.41	27.45	1.8030	1.1122	0.6782	0.428
	20.07	290.68	28.97	1.8688	1.1452	0.6717	0.413
	25.00	319.08	30.48	1.9271	1.1954	0.6667	0.402
Hydrocarbon gas	4.66	222.45	26.14	1.6469	1.0254	0.6895	0.449
	9.08	240.13	27.59	1.7154	1.0556	0.6855	0.440
	15.38	268.53	29.72	1.7788	1.0910	0.6793	0.431
	20.61	295.52	32.48	1.8424	1.1293	0.6732	0.420
	25.43	323.74	35.93	1.8922	1.1703	0.6682	0.412

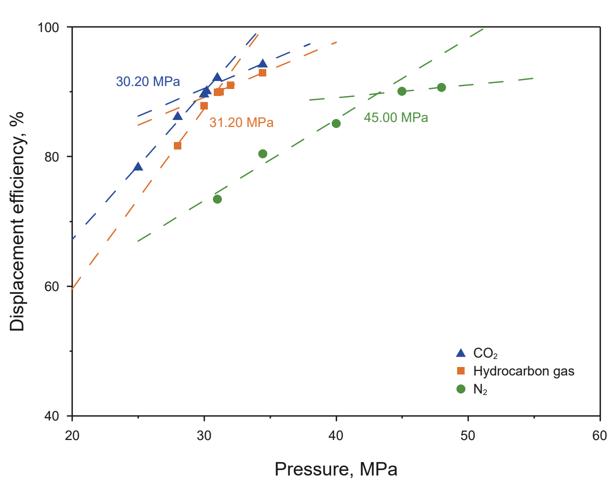

Fig. 2. Relationship between oil displacement efficiency and pressure in slim-tube experiments for different injection media.

The injection water was formulated based on the water quality analysis of produced water from the field. It is classified as $CaCl_2$-type formation water with a total salinity of 220,104 mg/L and a pH of 6.30. The mass concentrations of the major cations are Ca^{2+} (16,685 mg/L), Mg^{2+} (3189 mg/L), Sr^{2+} (690 mg/L), K^+ (900 mg/L), and Na^+ (61,500 mg/L), while the anions include Cl^- (136,898 mg/L), HCO_3^- (15 mg/L), and SO_4^{2-} (227 mg/L). To eliminate interference from formation water signals during the NMR oil displacement experiments, the injection water was prepared using heavy water (D_2O) as the solvent.

2.1.2. Core samples

For the NMR online oil displacement experiments, a core sample from the S-B3 formation was used, measuring 4.70 cm in length and 2.51 cm in diameter, with a permeability of 0.40×10^{-3} μm^2 and a porosity of 10.00%. To better represent the in-situ reservoir characteristics in the long-core flooding experiments, multiple short plug cores were assembled into a composite long core using the harmonic averaging method to determine the overall permeability. Filter papers were inserted between core segments to minimize capillary end effects (Wang et al., 2022). The final composite core measured 24.27 cm in total length, with an average porosity of 15.20% and an average permeability of 0.30×10^{-3} μm^2 (Table 3).

2.2. High-pressure and high-temperature (HPHT) online NMR displacement

2.2.1. Experiment apparatus

To investigate the distribution and behavior of crude oil in the pores under miscible and immiscible flooding conditions, a high-pressure and high-temperature (HPHT) online NMR gas flooding system was developed. The system consists of an injection pump unit, intermediate container, NMR core holder, back-pressure regulator, differential pressure transducer, temperature control system, and gas flowmeter (Fig. 3). A Ruska automatic displacement pump was employed to ensure precise flow control, with a speed accuracy of ±0.001 mL/min. The temperature control system maintains stability within ±0.1 °C, while the gas flowmeter provides a measurement accuracy of 0.1 mL. The magnetic field strength of the NMR scanner is 0.30 ± 0.05 T, ensuring stable and reliable signal acquisition under HPHT conditions.

Table 3
Physical parameters of experimental cores.

Experimental	Core number	Length, cm	Diameter, cm	Porosity, %	Permeability, 10^{-3} μm^2
NMR core displacement	/	4.70	2.51	10.00	0.40
Long core displacement	1 (exit)	6.64	3.76	11.00	0.32
	2	6.58	3.75	12.73	0.38
	3	4.86	3.78	21.08	0.19
	4 (entrance)	6.19	3.82	15.98	0.44

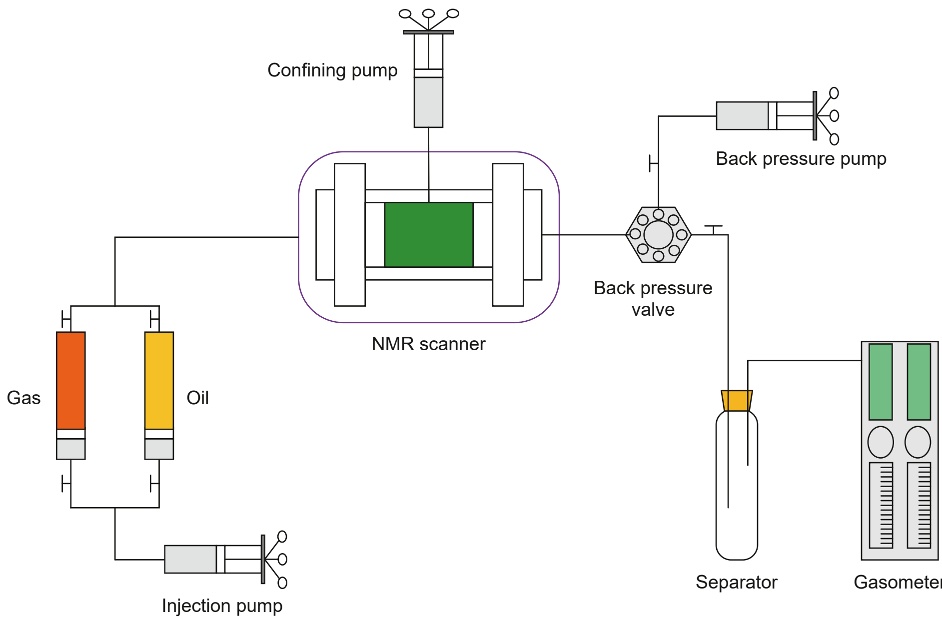

Fig. 3. Schematic diagram of the online nuclear magnetic resonance (NMR) displacement experimental apparatus.

2.2.2. Experimental procedure

(1) The core sample was evacuated and saturated with reconstituted reservoir crude oil, after which its NMR T_2 spectrum was measured. The core was then cleaned and dried to remove residual oil. (2) The dried core was placed in the NMR core holder, and heavy water (D_2O) was injected to raise the pore pressure to the initial reservoir pressure of 34.45 MPa. The system was subsequently heated to the reservoir temperature of 89 °C and held until pressure stabilization. Crude oil was then injected to displace the heavy water and establish irreducible water saturation. The displacement continued until the T_2 spectrum remained stable, and both the gas–oil ratio (GOR) and hydrocarbon composition at the outlet reached steady values. At this point, oil saturation was considered complete, and the corresponding NMR T_2 spectrum was recorded. (3) The gas injection phase was initiated by connecting the inlet to the selected injection gas. Gas flooding was conducted at a constant rate of 0.1250 mL/min, with the injected gas volume measured directly by the displacement pump. After every 0.2 hydrocarbon pore volume (HCPV) of gas injection (calculated as the injected gas volume divided by the original hydrocarbon pore volume of the core), an NMR T_2 scan was performed. Meanwhile, the produced oil volume, gas volume, and pressure differential between the inlet and outlet were continuously recorded. The experiment was terminated when no additional oil production was observed, marking the end of the displacement process.

2.3. Long core displacement experiment

2.3.1. Experiment apparatus

To investigate the effects of different injection media and gas injection parameters on oil displacement efficiency, a high-temperature and high-pressure (HTHP) long-core displacement system was developed (Cui et al., 2023). The apparatus is rated for a maximum pressure of 100 MPa and a maximum operating temperature of 150 °C. It consists of an injection pump system, intermediate transfer vessels, a long-core holder, a back-pressure regulator, a differential pressure gauge, a temperature control system, and a gas flowmeter. The instrument precision specifications are identical to those described in Section 2.2.1.

2.3.2. Experimental design and procedure

Based on the planned development strategy for the study area, ten long-core displacement experiments were designed (Table 4) to evaluate the effects of various injection media (CO_2, N_2, and hydrocarbon gas) and injection parameters (injection timing, rate, and method). Schemes 1–3: Optimization of injection media—continuous flooding using different gas types. Schemes 4–7: Parameter optimization for hydrocarbon gas injection—varying injection timing and rate. Schemes 8–10: Comparative experiments for different injection methods.

The experiments were conducted as follows: (1) The core was aged in degassed oil for 28 days, then cleaned, dried, and

Table 4
Experimental design for long-core physical simulation tests.

Experiment	Scheme	Injection media	Injection rate, mL·min^{-1}	Injection time, MPa		Injection method
Different injection media	1	N_2	0.1250	34.45		Continuous gas drive
	2	CO_2	0.1250	34.45		
	3	Hydrocarbon gas	0.1250	34.45		
Different injection parameter	4	Hydrocarbon gas	0.0625	31.00		Continuous gas drive
	5		0.0625	27.00		
	6		0.0625	Optimal gas injection timing for schemes 4 and 5		
	7		0.2500			
Different injection method	8	Hydrocarbon gas	0.1250	31.00		Pulse gas injection
	9	N_2	0.1250	27.00	0.1 PV Segment sealing	Huff and puff gas injection
	10	N_2	0.1250	27.00	0.2 PV Segment sealing	

assembled in the long-core holder using the harmonic averaging method to determine composite permeability. The system was evacuated to remove residual air. (2) The core was saturated with formation water, and the saturated water volume was recorded. The system was then pressurized to the initial reservoir pressure of 34.45 MPa, and after stabilization, heated to the reservoir temperature of 89 °C. (3) The core was saturated with degassed crude oil, and the volume of displaced water was recorded. The difference between the saturated water and displaced water volumes was used to calculate oil saturation. Reconstituted crude oil was then injected to replace the degassed oil until the gas–oil ratio (GOR) at the outlet was consistent with that reported in the PVT analysis. (4) Gas injection optimization tests were performed by continuously injecting gas at a constant rate until no further oil production was observed. The injected gas volume was measured directly using the displacement pump. After every 0.1 hydrocarbon pore volume (HCPV) of gas injection, the following parameters were recorded: produced oil volume, gas volume, differential pressure, confining pressure, and backpressure. (5) After each experiment, the core was cleaned sequentially with petroleum ether, toluene, and anhydrous ethanol, then dried with N_2 gas. Steps (2)–(5) were repeated for all subsequent injection parameter optimization experiments.

2.4. Methodological validation and limitations

The experimental design integrated high-temperature and high-pressure (HTHP) NMR online displacement experiments, long-core flooding tests, and numerical simulations, providing a comprehensive framework for evaluating gas flooding behavior in ultra-low-permeability carbonate reservoirs. The peculiarity of this methodology lies in the integration of real-time NMR monitoring with long-core dynamic displacement, enabling simultaneous observation of pore-scale fluid migration and macroscopic recovery performance under representative reservoir conditions (89 °C, salinity of 200,000 mg/L, and pressure up to 35 MPa).

During the experiments, strict temperature (±0.5 °C) and pressure (±0.2 MPa) control were maintained, and high-precision instruments were employed to ensure measurement accuracy. The reliability of the results was verified by the strong consistency among NMR displacement data, long-core flooding results, and numerical simulation outcomes, confirming the validity and reproducibility of the adopted methodology.

The present study was conducted under controlled laboratory conditions using core plugs of limited dimensions (2.5 cm in diameter and 10 cm in length). Consequently, heterogeneities at the field scale and capillary end effects may not be fully captured. Nevertheless, through the application of similarity theory, the injection–production parameters derived from laboratory-scale experiments can be scaled and translated to field conditions, allowing practical implementation in reservoir development.

3. Microscopic mechanism of mixed-phase oil displacement

3.1. Pore size distribution of rock samples

Under reservoir conditions of 34.45 MPa and 89 °C, the core sample saturated with reconstituted reservoir crude oil exhibited a tri-modal NMR T_2 spectrum. The dominant peak was observed within the 0.07–4.50 μm range, corresponding to the central peak position. The front peak represented pore sizes <0.07 μm, while the rear peak corresponded to pores >4.50 μm. The central peak displayed the highest amplitude and largest area, and the combined areas of the front and central peaks accounted for over 90% of the total spectral area. This indicates that pores smaller than 4.50 μm, particularly those within the 0.07–4.50 μm range, dominate the pore structure of the core. These sub-4.50 μm pores serve as the primary storage spaces for crude oil (Fig. 4).

3.2. (Non-)Miscible displacement of crude oil: differences in microscopic mobilization

At a reservoir pressure of 34.45 MPa and an injection rate of 0.1250 mL/min, miscibility markedly influenced both the overall oil mobilization efficiency and the mobilization behavior across different pore sizes during N_2 and CO_2 flooding. CO_2 miscible flooding achieved a total oil mobilization efficiency of 42.08%, exceeding that of N_2 immiscible flooding by approximately 10.00% (Fig. 5(c)). During N_2 flooding, oil mobilization primarily occurred in large pores (>4.50 μm), whereas CO_2 flooding effectively mobilized oil in both small (0.07–4.50 μm) and large pores

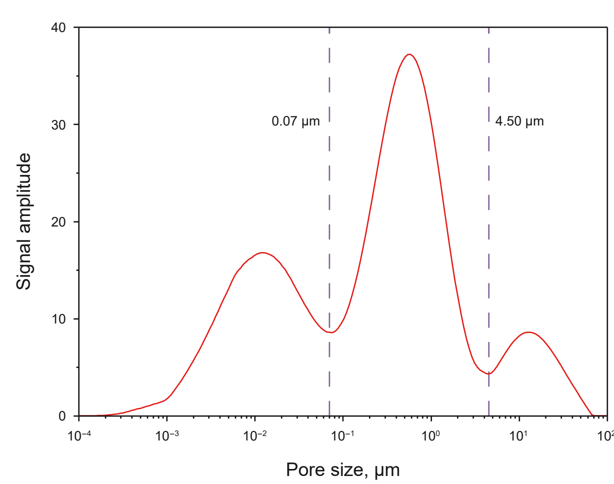

Fig. 4. NMR T_2 spectrum of the core saturated with reconstituted reservoir crude oil under reservoir conditions (34.45 MPa, 89 °C).

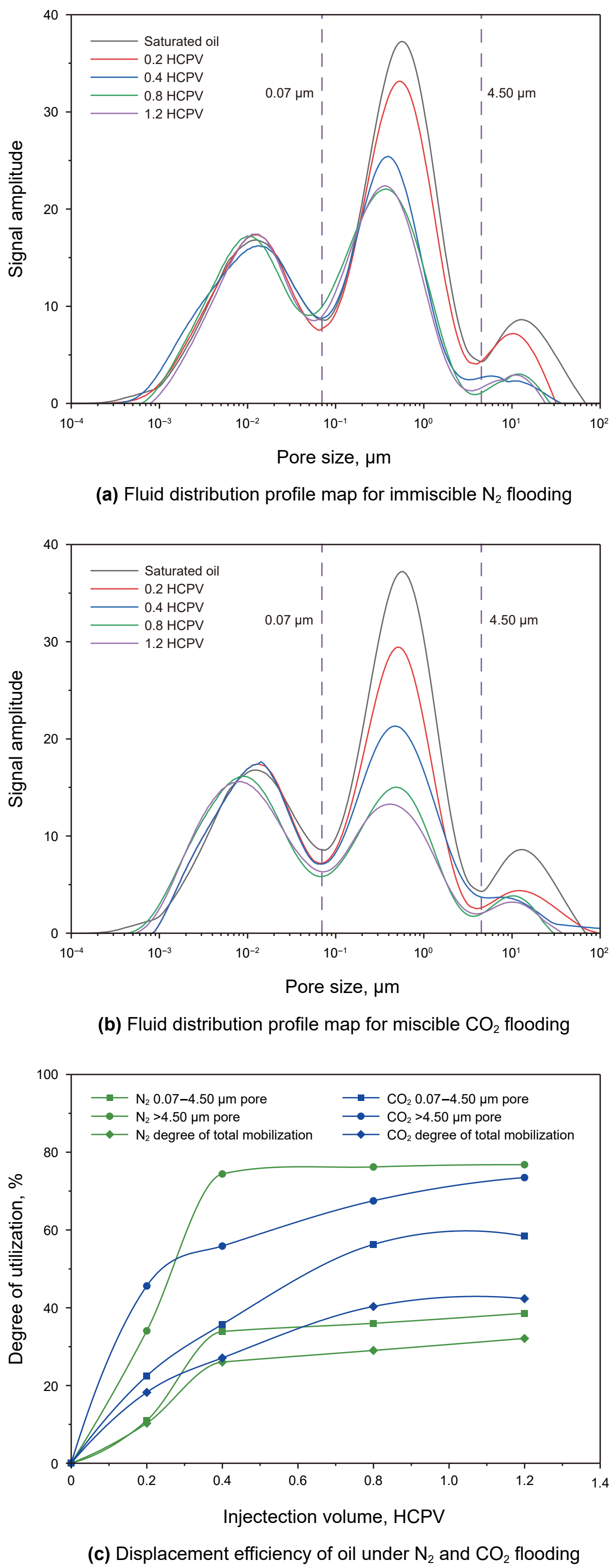

(a) Fluid distribution profile map for immiscible N_2 flooding

(b) Fluid distribution profile map for miscible CO_2 flooding

(c) Displacement efficiency of oil under N_2 and CO_2 flooding

Fig. 5. Fluid distribution and recovery state before and after gas injection displacement.

(>4.50 μm). However, neither N_2 nor CO_2 significantly mobilized oil in micro-pores (<0.07 μm) (Fig. 5(a) and (b)).

For large pores (>4.50 μm), CO_2 miscible and N_2 immiscible flooding yielded comparable mobilization efficiencies of 69.95% and 76.81%, respectively. However, in the early displacement stage (<0.4 HCPV), N_2 flooding achieved a higher efficiency of 74.39%, exceeding CO_2 flooding by 18.54% (Fig. 5(c)). This difference is attributed to the high solubility of CO_2 (Table 2), which leads to extensive dissolution into crude oil during the early phase. This dissolution reduces the amount of free CO_2 available for direct displacement, thereby weakening its sweeping effect in large pores. Consequently, N_2 flooding exhibits superior early-stage displacement efficiency in the macropore network.

For small pores (0.07–4.50 μm), CO_2 miscible flooding achieved an oil mobilization efficiency of 58.39%, nearly 20.00% higher than that of N_2 flooding. However, during the initial stage, both gases exhibited comparable performance (Fig. 5(c)), as early gas dissolution mainly occurred in large pores and had limited influence on smaller ones. With continued injection, CO_2"s high solubility and miscible displacement mechanism facilitated substantial dissolution into small-pore oil, enhancing elastic expansion and ultimately improving oil mobilization.

Overall, these results demonstrate that miscible flooding significantly enhances oil mobilization within small pores and substantially improves the overall displacement efficiency compared to immiscible flooding.

4. Effect of injected medium on oil displacement efficiency

A comparison of the experimental results from Schemes 1–3 demonstrates that the type of injection medium has a pronounced effect on the overall oil displacement efficiency. Under continuous gas injection at 34.45 MPa and an injection rate of 0.1250 mL/min, the gas breakthrough volumes for N_2, CO_2, and hydrocarbon gas were 0.5, 0.7, and 0.7 HCPV, respectively. The corresponding total displacement efficiencies were 47.28%, 75.52%, and 71.37%. The primary displacement stage occurred prior to gas breakthrough (Fig. 6).

Analysis indicates that both CO_2 and hydrocarbon gas achieved miscible flooding, resulting in delayed breakthrough compared with N_2 immiscible flooding. The prolonged main displacement stage under miscible conditions substantially improved overall recovery efficiency. In addition, the stronger swelling and viscosity reduction effects of CO_2 (Table 2) yielded a 4.15% higher displacement efficiency relative to hydrocarbon gas. These results clearly demonstrate that, for ultra-low-permeability carbonate reservoirs, miscible flooding with CO_2 or hydrocarbon gas significantly outperforms N_2 immiscible flooding, with CO_2 showing

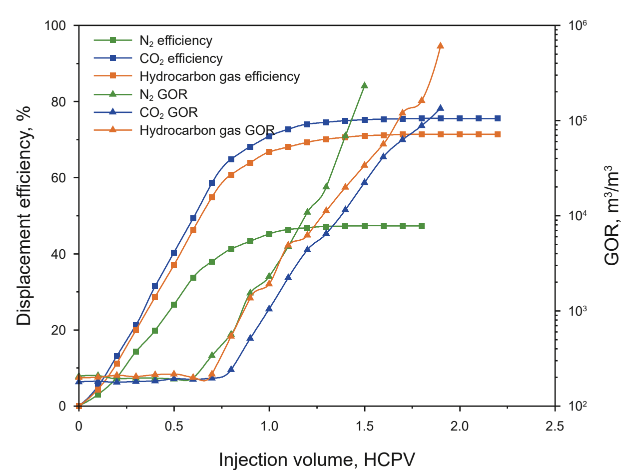

Fig. 6. Comparison of oil displacement efficiencies using different injection media under continuous gas injection.

slightly superior performance. However, considering field implementation feasibility, gas availability, and economic practicality, hydrocarbon gas is recommended as the preferred injection medium for reservoir development.

5. Effect of different gas injection parameters on oil displacement efficiency

5.1. Effect of gas injection parameters on oil displacement efficiency

5.1.1. Effect of gas injection timing on oil displacement efficiency

A comparison of Schemes 3, 4, and 5 highlights the influence of injection pressure on displacement performance during continuous hydrocarbon gas flooding. At injection pressures of 34.45, 31.00, and 27.00 MPa, the gas breakthrough volumes progressively decreased from 0.8 HCPV to 0.7 and 0.6 HCPV, respectively. The corresponding displacement efficiencies were 54.89%, 57.72%, and 50.03%, while the total recovery efficiencies declined from 72.28% to 66.27% and 52.47%, respectively. These results indicate that earlier gas injection timing, corresponding to higher reservoir pressures, significantly enhances oil recovery (Fig. 7).

Mechanistically, earlier gas injection ensures that the reservoir pressure remains above the minimum miscibility pressure (MMP) of hydrocarbon gas (31.20 MPa), thereby promoting miscible flooding and improving displacement effectiveness. Under such conditions, higher injection pressure enhances gas solubility in crude oil, leading to increased oil swelling, viscosity reduction, and improved fluid mobility, which collectively delay gas breakthrough. Furthermore, elevated injection pressures improve gas injectivity by enhancing compressibility and pore-scale expansion effects, which lower overall flow resistance and facilitate the displacement of resident liquid from the pore space. Consequently, these synergistic effects yield higher recovery factors at elevated pressures. The experimental results confirm that natural depletion results in poor recovery, whereas gas injection above the MMP achieves markedly superior performance. Overall, miscible flooding significantly outperforms immiscible flooding, demonstrating a clear dependence of recovery efficiency on injection pressure and miscibility conditions.

5.1.2. Effect of gas injection rate on oil displacement efficiency

The preceding section demonstrated that earlier gas injection timing enhances flooding performance. Accordingly, Schemes 6 and 7 were designed with injection initiated at 34.45 MPa and pressure maintained at 100% of the initial reservoir pressure. A comparison among Schemes 6, 3, and 7—conducted under the same reservoir pressure (34.45 MPa) but at different injection rates (0.0625, 0.1250, and 0.2500 mL/min)—showed that the gas breakthrough volumes advanced from 0.8 HCPV to 0.7 HCPV as the rate increased. The corresponding displacement efficiencies were 54.89%, 54.81%, and 59.91%, while the total recovery efficiencies decreased sequentially from 72.28% to 71.37% and 70.44%. These results indicate that overall flooding efficiency tends to decline with increasing injection rate (Fig. 8).

Mechanistically, the behavior of miscible gas flooding in ultra-low-permeability reservoirs differs from that observed in conventional formations. Although higher injection rates are often associated with improved sweep efficiency in traditional miscible flooding, ultra-tight reservoirs rely on multiple-contact miscibility (MCM) between the injected gas and crude oil. At elevated injection rates, the reduced gas–oil contact time limits interphase mass transfer, hindering the establishment of full miscibility and thereby diminishing flooding performance. Conversely, excessively low injection rates may lead to insufficient pressure maintenance, failing to overcome the threshold pressure gradient characteristic of such tight formations. Therefore, an optimal gas injection rate exists that balances pressure support and mass-transfer efficiency, ensuring the best miscible flooding performance in ultra-low-permeability carbonate reservoirs.

5.1.3. Effect of gas injection method on oil recovery efficiency

A comparative analysis was conducted between continuous gas injection (Scheme 4) and pulse gas injection (Scheme 8) under conditions where pressure decreased from 34.45 MPa to 31.00 MPa. In the pulse injection method, 0.1 pore volume (PV) of hydrocarbon gas was injected sequentially. After each injection, the inlet was closed to stabilize pressure, and the outlet was reopened to release gas until the system pressure returned to 31.00 MPa. Under these conditions, the oil displacement efficiency increased from 64.07% to 68.97%, with a delayed gas breakthrough observed for the pulse injection mode (Fig. 9). This improvement is attributed to the extended contact time between hydrocarbon gas and crude oil during pulse injection, which enhances interphase mass transfer, promotes more complete extraction, mitigates gas fingering, delays gas channeling, and ultimately improves recovery efficiency.

A similar comparison was performed for N_2 injection, involving continuous flooding (Scheme 1) and huff-and-puff injection

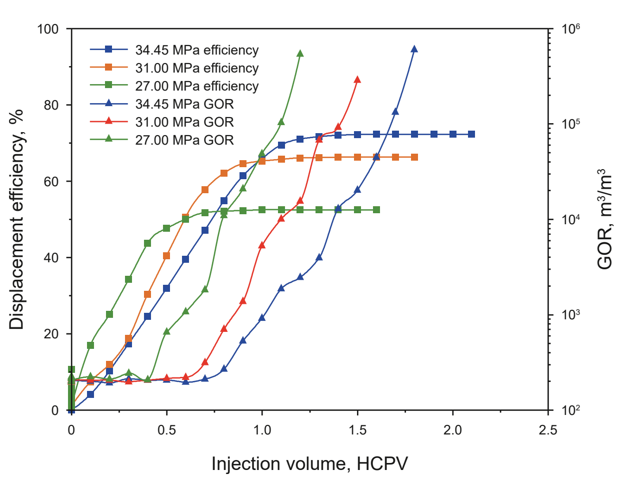

Fig. 7. Relationship between injected gas volume, oil recovery efficiency, and gas–oil ratio (GOR) for different injection timings of hydrocarbon gas.

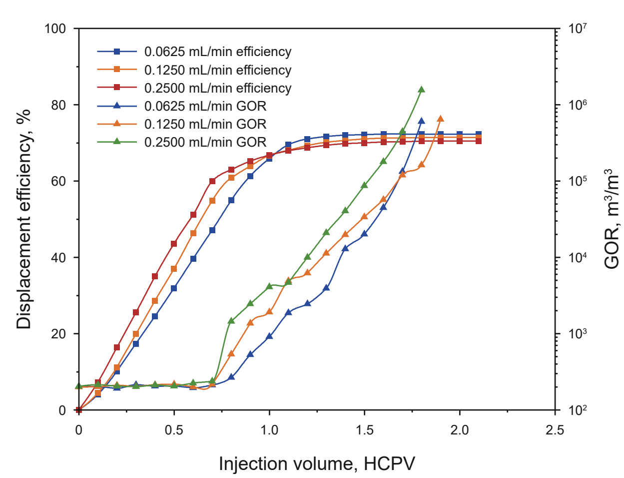

Fig. 8. Relationship between injected gas volume, oil recovery efficiency, and gas–oil ratio (GOR) for different injection rates of hydrocarbon gas.

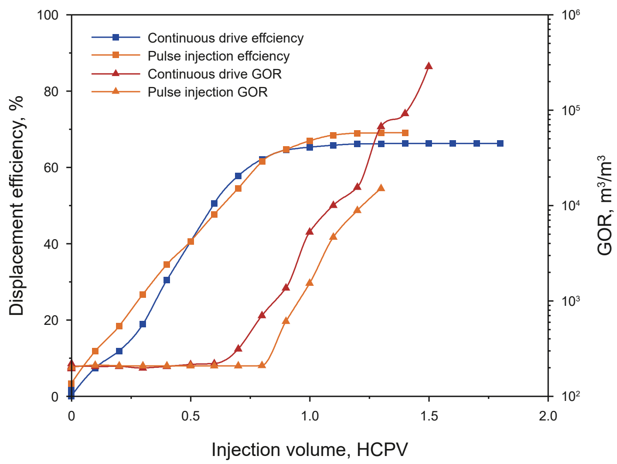

Fig. 9. Relationship between injected volume, oil recovery efficiency, and gas–oil ratio (GOR) for different injection methods of hydrocarbon gas.

(Schemes 9 and 10). In these experiments, N_2 was continuously injected at 34.45 MPa, then depleted to 27.00 MPa, followed by huff-and-puff injections with 0.1 PV and 0.2 PV slug sizes. The corresponding oil displacement efficiencies were 47.28%, 17.13%, and 18.45%, respectively (Fig. 10). Thus, the continuous N_2 flooding achieved nearly 30.00% higher recovery than the huff-and-puff methods. The superior performance of continuous N_2 flooding can be attributed to two main mechanisms: (1) Higher injection pressure enhances the dissolution of N_2 into crude oil, improving swelling and viscosity reduction. (2) Continuous gas injection rapidly replenishes formation energy, allowing free-phase N_2 to effectively displace the residual oil. These findings demonstrate that, under immiscible conditions, continuous N_2 flooding outperforms huff-and-puff injection by nearly 30% in overall recovery efficiency.

5.2. Gas injection parameter sensitivity analysis

The experimental results presented above indicate that both injection rate and injection timing exert significant influences on the oil recovery efficiency of ultra-low-permeability porous carbonate reservoirs. Due to the extremely low permeability, fluid flow within such reservoirs exhibits non-Darcy behavior at the macroscopic scale, characterized by a distinct threshold pressure gradient (Chi et al., 2017). At the microscopic scale, gas from larger pores diffuses into smaller pore throats under the action of this pressure gradient (Tan et al., 2022), promoting oil mobilization through molecular diffusion and mass transfer. The coupled effects of gas diffusion–mass transfer and the threshold pressure gradient jointly control the final recovery efficiency.

To verify the existence of optimal injection timing and rate, a representative core from the S-B3 layer—with physical properties closely matching those of the composite long core—was selected. The core was 6.64 cm in length, 3.76 cm in diameter, and had a permeability of 0.32 × 10^{-3} μm^2. Using the bubble method, the threshold pressure gradient was determined to be 0.624 MPa/m.

A numerical simulation model was then developed to replicate the physical properties and experimental conditions of the core displacement tests. The model adopted an orthogonal grid system (100 × 1 × 1) with a grid size of 0.24 cm × 3.37 cm × 3.37 cm. The initial oil saturation was set at 68.00%, and the crude oil was divided into seven pseudo-components: N_2, CO_2, C_1, C_2, C_3, iC_4–C_6, and C_7^+. Based on phase behavior calibration (Figs. 11–13) and core flooding history matching, the model was used to further evaluate the effects of injection rate and timing on oil recovery in ultra-low-permeability porous carbonate reservoirs.

5.2.1. Injection timing sensitivity analysis

Recovery efficiencies for N_2, CO_2, and hydrocarbon gas were evaluated across seven injection timings at a fixed injection rate of 0.1250 mL/min (Fig. 14). For N_2 immiscible flooding, recovery efficiency declined sharply when the injection pressure dropped below the crude oil bubble point pressure (24.51 MPa), primarily due to gas exsolution, increased oil viscosity, and multiphase flow resistance. In contrast, during miscible flooding (CO_2 and hydrocarbon gas), displacement efficiency decreased once the injection pressure fell below the minimum miscibility pressure (MMP: 31.20 MPa), as delayed phase miscibility hindered effective oil mobilization. These findings highlight the importance of maintaining reservoir pressure above 72% of the initial pressure (≥24.51 MPa) for N_2 immiscible flooding and above 90% (≥31.20 MPa) for miscible gas flooding to ensure optimal oil recovery.

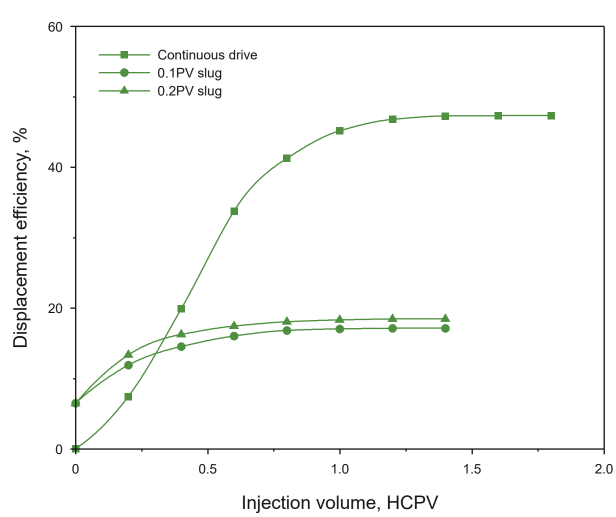

Fig. 10. Comparison of oil recovery efficiencies between continuous and huff-and-puff N_2 injection methods.

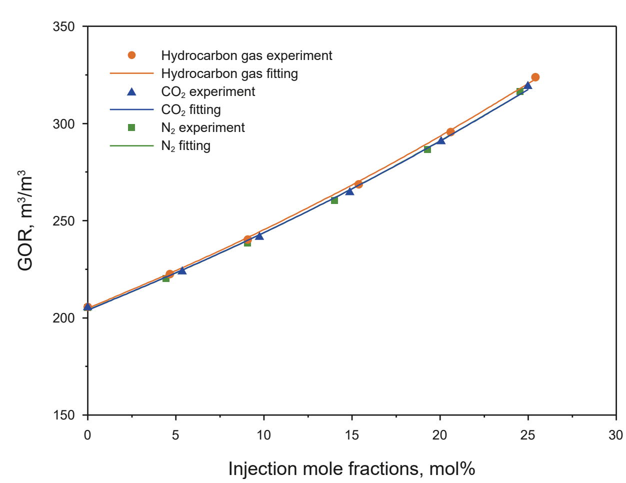

Fig. 11. Gas–oil matching curve from gas injection expansion tests.

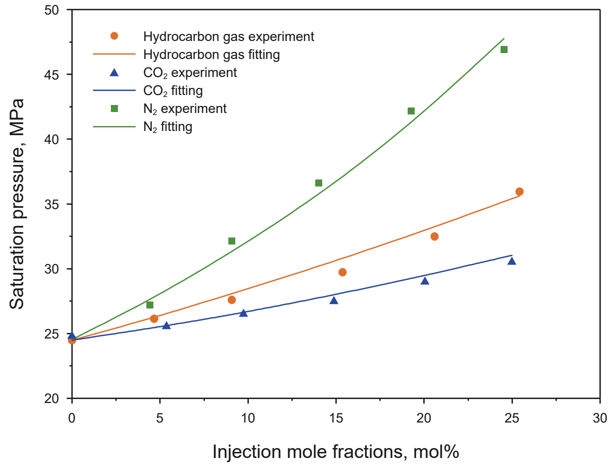

Fig. 12. Saturation pressure fitting from gas injection expansion tests.

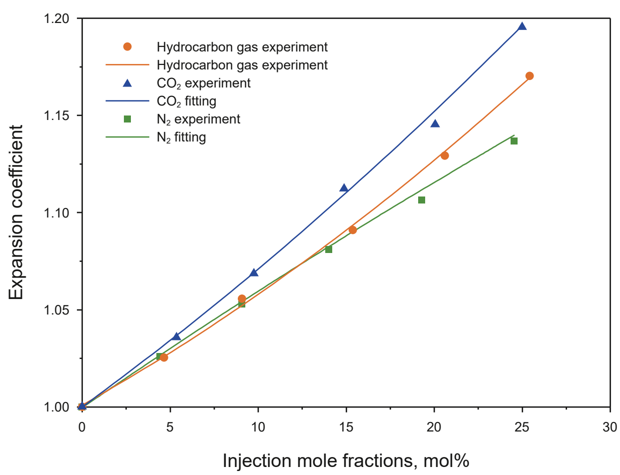

Fig. 13. Oil expansion coefficient fitting from gas injection expansion tests.

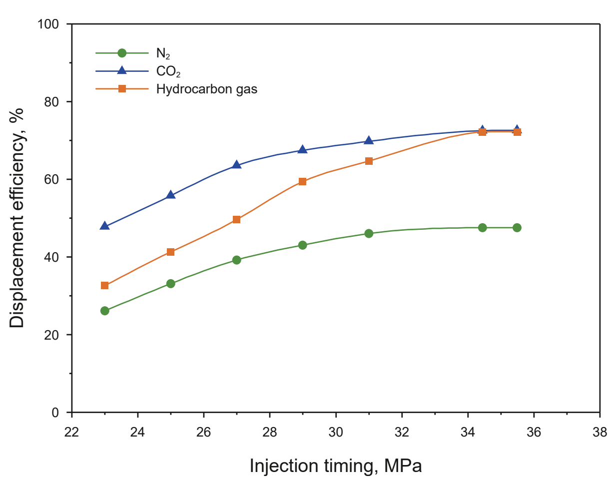

Fig. 14. Sensitivity analysis results for different gas injection timings.

5.2.2. Injection rate sensitivity analysis

At a constant reservoir pressure of 34.45 MPa, the peak recovery efficiencies for N_2, CO_2, and hydrocarbon gas were observed at injection rates of 0.0500 mL/min (48.56%), 0.0625 mL/min

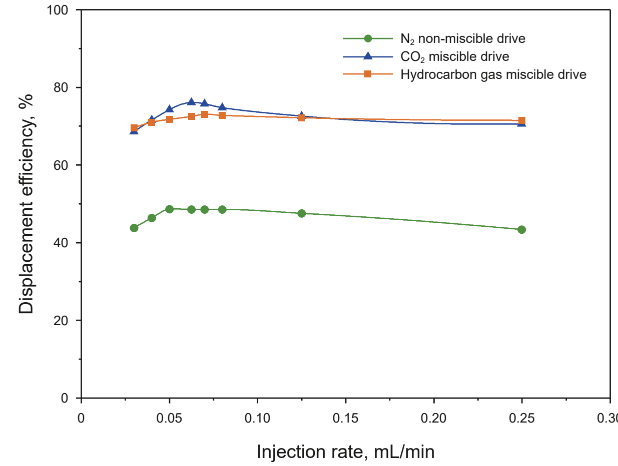

Fig. 15. Sensitivity analysis results for injection rates under miscible and immiscible flooding.

(76.04%), and 0.0700 mL/min (73.02%), respectively (Fig. 15). Deviations from these optimal rates led to a decline in displacement efficiency, confirming the existence of rate-dependent optimization for ultra-low-permeability reservoirs. In miscible flooding, slower injection rates promote gas–oil mass transfer but reduce pressure maintenance, whereas faster rates maintain pressure but limit contact time. For immiscible N_2 flooding, optimizing the balance between gas dissolution and pressure support is essential to maximize recovery.

In the S reservoir, miscible flooding (CO_2 or hydrocarbon gas) proceeds through a multiple-contact miscibility (MCM) process, whereby the injected gas gradually extracts heavier oil components or enriches the oil with light components from the gas until phase equilibrium is achieved (Song et al., 2024b). As gas injection continues, gas molecules diffuse from larger pores into smaller throats, promoting interphase mixing and mass transfer (Tan et al., 2022). In miscible displacement, molecular diffusion between gas and oil eventually reaches equilibrium, while in immiscible N_2 flooding, diffusion-driven mass transfer still enhances crude oil mobility through partial equilibrium mechanisms. However, injection rate optimization involves a critical trade-off: Lower rates extend gas–oil contact time, improving mass transfer but reducing average formation pressure, thereby limiting the ability to overcome the threshold pressure gradient; Higher rates maintain formation pressure but shorten contact time, constraining diffusion and reducing recovery.

The interplay between molecular diffusion and the threshold pressure gradient ultimately controls the overall recovery efficiency in the S reservoir. These mechanisms explain the distinct recovery trends observed in miscible (hydrocarbon gas) and immiscible (N_2) flooding (Figs. 16 and 17). Hydrocarbon gas miscible flooding achieved recovery efficiencies exceeding 60%, while N_2 immiscible flooding attained approximately 40%. Higher levels of pressure maintenance correlate positively with displacement efficiency, as gas injection simultaneously overcomes the threshold pressure gradient and enhances gas–oil mass transfer. The optimal injection rates, ensuring a balance between pressure support and diffusion effectiveness, were determined to be 0.0700 mL/min for hydrocarbon gas and 0.0500 mL/min for N_2.

5.2.3. Injection-production ratio sensitivity analysis

To further validate the rationality of the optimized injection rate and recovery performance, sensitivity analyses were conducted for N_2, CO_2, and hydrocarbon gas at their respective

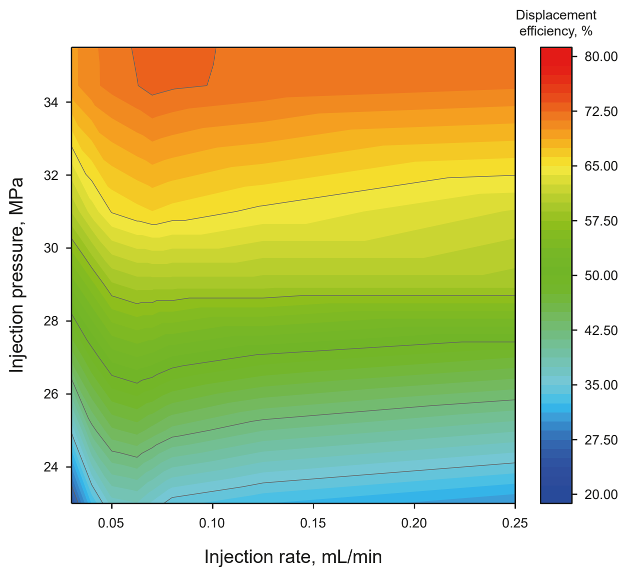

Fig. 16. Oil recovery efficiency as a function of injection rate and timing for hydrocarbon gas miscible flooding.

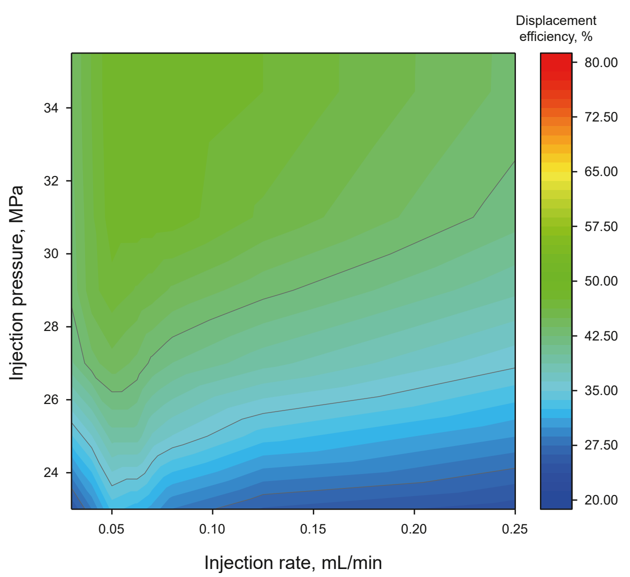

Fig. 17. Oil recovery efficiency as a function of injection rate and timing for N_2 immiscible flooding.

optimal injection rates of 0.0500 mL/min, 0.0625 mL/min, and 0.0700 mL/min, while maintaining a constant total injection volume of 1.2 HCPV. The oil displacement efficiency under different injection–production ratios was calculated (Fig. 18). For CO_2 and hydrocarbon gas, the highest recovery factors—76.18% and 73.46%, respectively—were achieved at an injection–production ratio of 1:1. In contrast, N_2 attained its peak displacement efficiency of 48.52% at a ratio of 1:1.2, indicating that immiscible flooding requires slightly higher injection volumes to maintain displacement pressure and sustain effective gas drive.

5.3. Recommended development strategy for the S reservoir

The S reservoir demonstrates markedly improved pore-scale oil utilization and overall recovery efficiency through miscible gas

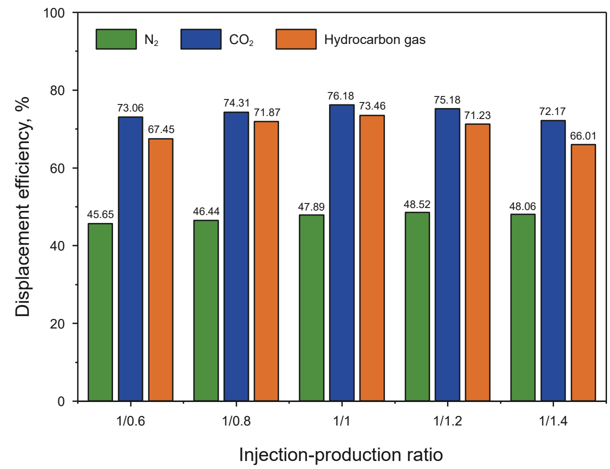

Fig. 18. Relationship between gas-to-oil ratio and oil recovery efficiency for different injection media.

flooding (CO_2 or hydrocarbon gas) compared with N_2 immiscible flooding. Under continuous injection at 34.45 MPa and 0.1250 mL/min, miscible flooding mobilized approximately 20% more crude oil in small pores (0.07–4.50 μm) than N_2 flooding (Fig. 5). Increased injection pressure further enhanced displacement efficiency, with recovery showing a positive correlation with pressure levels (Fig. 7). The coupling of threshold pressure gradient and molecular diffusion effects necessitates an optimal gas injection rate (Fig. 8), while pulse injection improves recovery by prolonging gas–oil contact and enhancing mass transfer (Fig. 9).

Although CO_2 exhibited slightly higher displacement efficiency, hydrocarbon gas is recommended as the preferred injection medium due to its lower cost, wide availability, and greater operational feasibility in field applications. For ultra-low-permeability carbonate reservoirs analogous to the S reservoir, the optimal development strategy involves continuous or pulse miscible flooding conducted at pressures exceeding the minimum miscibility pressure (MMP). Under such conditions, a laboratory-derived optimal injection rate of 0.0700 mL/min—equivalent to approximately 0.0908 m/d when scaled to field dimensions based on the core outlet cross-section—ensures a balanced interplay between pressure maintenance and diffusion-driven mass transfer. An injection-to-production ratio of 1:1 is recommended to maximize displacement efficiency. This integrated approach effectively harmonizes macroscopic flow control with microscopic diffusion mechanisms, thereby enhancing overall oil recovery performance in ultra-low-permeability carbonate reservoirs.

6. Conclusions

In this study, high-temperature and high-pressure NMR online displacement experiments, long-core flooding tests, and numerical simulations were integrated to investigate the gas flooding performance and controlling mechanisms of ultra-low-permeability porous carbonate reservoirs such as the S reservoir. The main conclusions are as follows.

(1) Gas injection significantly enhances crude oil recovery in ultra-low-permeability porous carbonate reservoirs by improving the elastic expansion capacity of crude oil. Under current formation pressure conditions (34.45 MPa), both CO_2 and hydrocarbon gas achieve miscible flooding, increasing the utilization of crude oil in small pores (0.07–4.50 μm) by approximately 20.00% compared with

immiscible flooding. In contrast, N_2 remains immiscible, yielding a maximum recovery of 18.41% at an optimal injection rate of 0.0500 mL/min and a slug size of 0.2 HCPV.

(2) The performance of miscible flooding is strongly influenced by reservoir pressure and injection rate. For hydrocarbon gas and CO_2, maintaining reservoir pressure at 88.00%–91.00% of the initial pressure (i.e., above the minimum miscibility pressure, MMP) and adopting an injection rate of 0.0811–0.0908 m/d result in the highest oil recovery efficiencies of 73.00%–76.00%. Pulse gas injection further extends gas–oil contact time, enhancing recovery by 4.92% relative to continuous flooding. Overall, miscible flooding surpasses immiscible displacement by mobilizing small-pore oil, delaying gas breakthrough, and increasing recovery efficiency by 24.09%–28.24%.

(3) The coupling between molecular diffusion and the critical threshold pressure gradient is identified as the dominant mechanism controlling gas flooding behavior in ultra-low-permeability carbonate reservoirs. This coupling governs both macroscopic non-Darcy flow and microscopic diffusion-driven displacement, offering new insights into the mechanisms that determine gas injection efficiency.

(4) Practical application and engineering implications: The injection–production parameters derived under laboratory conditions cannot be directly applied to field-scale reservoirs due to differences between linear and radial flow systems. These parameters should be translated to field operations using similarity theory, considering reservoir characteristics and production constraints. Moreover, engineering challenges associated with CO_2 injection—such as corrosion of steel components, cement degradation, and wellbore integrity concerns—must be carefully managed to ensure safe and sustainable implementation of CO_2-based enhanced oil recovery (EOR) (Khormali and Ahmadi, 2023; Khormali et al., 2025).

CRediT authorship contribution statement

Zhou-Hua Wang: Writing – review & editing. **Xin-Tong Zhang:** Writing – original draft, Conceptualization. **Guang-Ya Zhu:** Project administration, Funding acquisition. **Ping Guo:** Supervision, Project administration. **Nan Li:** Project administration, Funding acquisition. **Hui Liu:** Project administration, Conceptualization. **Zhao-Ming Li:** Validation. **Huang Liu:** Supervision, Project administration. **Shuo-Shi Wang:** Project administration.

Declaration of competing interest

The authors declare that they have no known competing financial interests or personal relationships that could have appeared to influence the work reported in this paper.

Acknowledgments

This work was supported by the China National Petroleum Corporation's "14th Five-Year Plan" forward-looking basic major scientific and technological project "Research on Key Technologies for Economic and Effective Development of Ultra-Low Permeability Carbonate Reservoirs" (2021DJ3202).

References

Abedini, A., Torabi, F., Mosavat, N., 2015. Performance of immiscible and miscible CO_2 injection process in a tight carbonate reservoir (experimental and simulation approach). Int. J. Oil Gas Coal Technol. 9 (3), 265–279. https://doi.org/10.1504/ijogct.2015.068994.

Al-Hadhrami, A., Davis, D., Deinum, G., 2007. The design of the first miscible sour gasflood project in Oman. In: International Petroleum Technology Conference, IPTC-11396-MS. https://doi.org/10.2523/iptc-11396-MS.

Al-Hajeri, S., Negahban, S., Al-Yafei, G., et al., 2010. Design and implementation of the first CO_2-EOR pilot in Abu Dhabi, UAE. In: SPE EOR Conference at Oil & Gas West Asia, SPE-129609-MS. https://doi.org/10.2118/129609-ms.

Al-Murayri, M.T., Kamal, D.S., Al-Sabah, H.M., et al., 2019. Low-salinity polymer flooding in a high-temperature low-permeability carbonate reservoir in west Kuwait. In: SPE Kuwait Oil & Gas Show and Conference, SPE-198000-MS. https://doi.org/10.2118/198000-MS.

Al-Riyamy, Q., Kelly, S., Al-Rawahi, A., et al., 2005. Precambrian field Oman from greenfield to EOR. In: SPE Middle East Oil and Gas Show and Conference, SPE-93364-MS. https://doi.org/10.2118/93364-ms.

Chi, J., Ju, B.S., Lyu, G.Z., et al., 2017. A computational method of critical well spacing of CO_2 miscible and immiscible concurrent flooding. Petrol. Explor. Dev. 44 (5), 815–823. https://doi.org/10.1016/s1876-3804(17)30092-7.

Choubineh, A., Helalizadeh, A., Wood, D.A., 2019. The impacts of gas impurities on the minimum miscibility pressure of injected CO_2-rich gas–crude oil systems and enhanced oil recovery potential. Pet. Sci. 16 (1), 117–126. https://doi.org/10.1007/s12182-018-0256-8.

Cui, X.D., Liao, H.Q., Chen, D.P., et al., 2023. Experiments about retrograde condensate pollution characteristics and relief measures in Fengshen 1 condensate gas reservoir with low permeability. Pet Geol; Recovery Efficiency 30 (6), 160–166. https://doi.org/10.13673/j.pgre.202211006 (in Chinese).

Deinum, G., Dindoruk, B., O' Dell, M., 2007. Gas blending for miscible gasfloods in south Oman. In: SPE Middle East Oil & Gas Show and Conference, SPE-105604-MS. https://doi.org/10.2118/105604-MS.

Figuera, L., Al-Hammadi, K., Tanakov, M., 2016. Case study of CO_2 injection to enhance oil recovery into the transition zone of a tight carbonate reservoir. In: Abu Dhabi International Petroleum Exhibition & Conference, SPE-183203-MS. https://doi.org/10.2118/183203-MS.

Han, H.S., Li, S.S., Yao, X.Q., et al., 2018. Swelling ability prediction method of crude oil-CO_2 system based on molar density. Acta Pet. Sin. 39 (4), 456–462. https://doi.org/10.7623/syxb201804009 (in Chinese).

Han, H.S., Yuan, S.Y., Li, S., et al., 2015. Dissolving capacity and volume expansion of carbon dioxide in chain n-alkanes. Petrol. Explor. Dev. 42 (1), 97–103. https://doi.org/10.1016/s1876-3804(15)60011-8.

Hu, W., Lü, C., Wang, R., et al., 2018. Porous flow mechanisms and mass transfer characteristics of CO_2 miscible flooding after water flooding. Acta Pet. Sin. 39 (2), 201–207. https://doi.org/10.7623/syxb201802008 (in Chinese).

Ju, B.S., Wu, Y.S., Qin, J.S., et al., 2012. Modeling CO_2 miscible flooding for enhanced oil recovery. Pet. Sci. 9 (2), 192–198. https://doi.org/10.1007/s12182-012-0199-4.

Keyvani, F., Safaei, A., Kazemzadeh, Y., et al., 2024. Impact of nanopore confinement on phase behavior and enriched gas minimum miscibility pressure in asphaltenic tight oil reservoirs. Sci Rep-Uk 14 (1), 13405. https://doi.org/10.1038/s41598-024-64194-2.

Khormali, A., Ahmadi, S., 2023. Synergistic effect between oleic imidazoline and 2-mercaptobenzimidazole for increasing the corrosion inhibition performance in carbon steel samples. Iranian J Chem; Chem Eng—Int English Ed 42 (1), 321–336. https://doi.org/10.30492/ijcce.2022.546098.5091.

Khormali, A., Ahmadi, S., Kazemzadeh, Y., et al., 2025. Evaluating the efficacy of binary benzimidazole derivatives as corrosion inhibitors for carbon steel using multi-modal analysis and optimization techniques. Results Eng. 26, 104671. https://doi.org/10.1016/j.rineng.2025.104671.

Li, Y., Zhang, Q., Wang, D.G., et al., 2020. A fast method of waterflooding performance forecast for large-scale thick carbonate reservoirs. J. Pet. Sci. Eng. 192, 107227. https://doi.org/10.1016/j.petrol.2020.107227.

Li, Z.M., Husein, M., Hemmati-Sarapardeh, A., 2022. Gas Injection Methods. Gulf Professional Publishing RM, pp. 133–169.

Liu, H., Dong, J.C., Liu, Y., et al., 2013. Experiments on gas and water injection for enhanced oil recovery in porous carbonate reservoir. J China Univers Pet (Ed Nat Sci) 37 (1), 104–108. https://doi.org/10.3969/j.issn.1673-5005.2013.01.017 (in Chinese).

Liu, X.L., Qin, J.S., Han, H.S., et al., 2017. Multiphase boundary of C_{16+} heavy n-alkanes and CO_2 systems. Petrol. Explor. Dev. 44 (1), 105–110. https://doi.org/10.1016/s1876-3804(17)30013-7.

Liu, Y.Z., Chen, X.L., 2010. Miscible conditions of CO_2 flooding technology used in low permeability reserviors. Petrol. Explor. Dev. 37 (4), 1849-0. https://www.sciengine.com/doi/10.0000/1000-0747-37-1849.

Mogensen, K.S., Masalmeh, S.K., 2020. A review of EOR techniques for carbonate reservoirs in challenging geological settings. J. Petrol. Sci. Eng. 195, 107889. https://doi.org/10.1016/j.petrol.2020.107889.

Mohammadi, M., Nikbin-Fashkacheh, H., Mahani, H., 2022. Pore network-scale visualization of the effect of brine composition on sweep efficiency and speed of oil recovery from carbonates using a photolithography-based calcite microfluidic model. J. Petrol. Sci. Eng. 208 (Part D), 109641. https://doi.org/10.1016/j.petrol.2021.109641.

Saadawi, H., 2010. Surface facilities for a CO_2-EOR project in Abu Dhabi. In: SPE EOR Conference at Oil & Gas West Asia, SPE-127765-MS. https://doi.org/10.2118/127765-ms.

Safaei, A., Kazemzadeh, Y., Riazi, M., 2021. Mini review of miscible condition evaluation and experimental methods of gas miscible injection in conventional

and fractured reservoirs. Energy Fuels 35 (9), 7340–7363. https://doi.org/10.1021/acs.energyfuels.0c04384.
Salma, A.-H., Ghedan, S., Al-Basry, A., 2011. Integrated history matching simulation study of the first miscible CO_2-EOR pilot in Abu Dhabi heterogeneous carbonate oil reservoir. In: SPE Middle East Oil and Gas Show and Conference, SPE-142623-MS. https://doi.org/10.2118/142623-MS.
Shi, X.W., Yang, Z.M., Zhang, Y.P., et al., 2017. Physical simulation of colayer water flooding in low permeability carbonate reservoir in Middle East. J. Eng. 2017 (1), 2510251. https://doi.org/10.1155/2017/2510251.
Song, X.M., Li, Y., 2018. Optimum development options and strategies for water injection development of carbonate reservoirs in the Middle East. Petrol. Explor. Dev. 45 (4), 723–734. https://doi.org/10.1016/S1876-3804(18)30075-2.
Song, X.M., Li, Y., Li, F.F., et al., 2024a. Separate-layer balanced waterflooding development technology for thick and complex carbonate reservoirs in the Middle East. Petrol. Explor. Dev. 51 (3), 661–673. https://doi.org/10.1016/s1876-3804(24)60495-7.
Song, Z.J., Deng, S., Song, Y.,L., et al., 2024b. High-pressure phase behavior and mass transfer law of Gulong shale oil and CO_2 in Daqing oilfield. Acta Pet. Sin. 45 (2), 390–402. https://doi.org/10.7623/syxb202402005 (in Chinese).
Su, H.Y., Liao, C.L., 2014. Oil displacement experiment for enhancing oil recovery of porous type carbonate reservoir. Electron. J. Geotech. Eng. 19 (Z4), 16857–16868.
Sun, L.F., Li, Y., Li, B.Z., 2022. Classified evaluation methods and waterflood development strategies for carbonate reservoirs in the Middle East. Acta Pet. Sin. 43 (2), 270–280. https://doi.org/10.7623/syxb202202009 (in Chinese).
Tan, Y.S., Li, Q., Xu, L., et al., 2022. A critical review of carbon dioxide enhanced oil recovery in carbonate reservoirs. Fuel 328 (Suppl. C), 125256. https://doi.org/10.1016/j.fuel.2022.125256.
Wan, T., Liu, H.X., 2018. Exploitation of fractured shale oil resources by cyclic CO_2 injection. Pet. Sci. 15 (3), 552–563. https://doi.org/10.1007/s12182-018-0226-1.
Wang, Y.L., Song, X.M., Wang, G.H., et al., 2020. Key technologies and practices for rapid and large-scale production increase in cooperation oil and gas fields of the Middle East. Acta Pet. Sin. 41 (12), 1633–1642. https://doi.org/10.7623/syxb202012015 (in Chinese).
Wang, Z.H., Wang, T., Liu, H., et al., 2022. Experimental study of the development mode of gas-cap edge-water reservoir:a case study of Khasib reservoir of Halfaya oilfield in Iraq. Petrol. Explor. Dev. 49 (3), 625–635. https://doi.org/10.1016/S1876-3804(22)60052-1.
Wei, C.J., Li, Z.H., Yang, J., et al., 2022. A comprehensive performance evaluation methodology for miscible gas flooding: A case study in a giant carbonate reservoir in Middle East. J. Petrol. Sci. Eng. 215 (Part B), 110668. https://doi.org/10.1016/j.petrol.2022.110668.
Yang, J.J., Yagna Deepika, O., Karam, P., et al., 2017. Miscible CO_2 flooding using horizontal multi-fractured wells in the San Andres Formation, TX – A feasibility study. In: Carbon Management Technology Conference, CMTC-486335-MS. https://doi.org/10.7122/486335-MS.
Yang, J., Liu, H., Ning, C.Z., 2022a. Adaptability and optimal design of stimulation measures of low permeability carbonate reservoirs. PetroChina Res Inst Pet Explor; Development, Beijing 7 (2), 204–212. https://doi.org/10.3969/j.issn.2096-1693.2022.02.018, 100083, China.
Yang, J., Zhu, G.Y., An, Y.C., et al., 2022b. Integrated reservoir model and differential stimulation modes of low permeability porous carbonate reservoir: A case study of S reservoir in X Oilfield in Iraq. Processes 10 (6), 1179. https://doi.org/10.3390/pr10061179.
Yu, H.Y., Yang, Z.L., Liu, J.H., et al., 2019. EOR method by the carbonated water injection (CWI) for tight oil reservoirs. Pet. Geol. Oilfield Dev. Daqing 38 (2), 166–174. https://doi.org/10.19597/j.Issn.1000-3754.201807019 (in Chinese).
Yuan, S.Y., Wang, Q.F., Li, J.S., et al., 2020. Technology progress and prospects of enhanced oil recovery by gas injection. Acta Pet. Sin. 41 (12), 1623–1632. https://doi.org/10.7623/syxb202012014 (in Chinese).
Zhang, Y.P., Yang, Z.M., Huang, Y.Z., et al., 2021. Study on reservoir characteristics and remaining oil distribution of low permeability pore type carbonate rock. J. Jilin Univ. (Earth Sci. Ed.) 51 (3), 659. https://doi.org/10.13278/j.cnki.jjuese.20200094 (in Chinese).
Zhu, C.F., Guo, W., Wang, Y.P., et al., 2021. Experimental study of enhanced oil recovery by CO_2 huff-n-puff in shales and tight sandstones with fractures. Pet. Sci. 18 (3), 852–869. https://doi.org/10.1007/s12182-020-00538-7.